PHYSICAL REVIEW B VOLUME 24, NUMBER 4 15 AUGUST 1981

Phonon polariton study of $CuCl_{1-x}Br_x$

G. Livescu, Z. Vardeny,* and O. Brafman
Physics Department and Solid State Institute, Technion-Israel Institute of Technology, Haifa, Israel
(Received 9 February 1981)

The optical-phonon spectrum of $CuCl_{1-x}Br_x$ at low temperature is very unusual in regard to many of its properties. Despite the apparent two-mode behavior our measurements illustrate anomalies in the Raman intensity and temperature-induced frequency shift, as well as in the oscillator strengths yielded by the polariton measurements. All these irregularities are connected to the anomalies of CuCl and they disappear rapidly with increasing Br concentration. The data are interpreted in terms of a previous model, which allows copper ions to occupy off-center sites. It is assumed that in $CuCl_{1-x}Br_x$ this may happen only in the tetrahedra where Cu^+ is surrounded by chlorine ions alone.

I. INTRODUCTION

We shall be dealing here with the oddly behaved polar phonon modes in $CuCl_{1-x}Br_x$ solid solutions at low temperatures. These are tightly connected to the properties and anomalous phenomena of the pure substances in this temperature region, which will be briefly reviewed first. Copper halides are of zinc-blende structure with two atoms per unit cell and therefore should have a single polar mode in this phase. Despite this, two polar modes are found in the optic-phonon spectrum of CuCl even at very low temperature.[1-10] These polar modes, labeled β and γ, exhibit the same symmetry but are very different as to their linewidth and the effect temperature has on their frequency, intensity, and linewidth.[2,3] In CuBr similar phenomena were observed,[11,12] but as we restrict our study to low temperatures only ($T \leq 11$ K) nothing unusual is detected in the phonon spectrum of CuBr at these temperatures.

One attempt to account for the anomaly in CuCl was based on a Ruvalds-Zawadowski type of interaction between the TO phonon and a background of acoustic two-phonon combination.[5] A second approach, the one to which we shall refer later, assumes the possibility of four equivalent secondary minima in the copper ion potential. Thus, in addition to the ideal sites at the center of the Cl^- tetrahedra, Cu^+ may occupy off-center sites. This gives rise to two different optical-phonon modes: one due to Cu^+ at ideal sites (γ) and the other due to Cu^+ at off-center sites (β). Again, in CuBr a similar phenomenon occurs, but only at higher temperatures.[8] A full description of this model and its wide experimental basis are given in Refs. 8–10. With this great difference between the optic phonons of CuCl and CuBr at low temperature it is only natural to study the phonon spectra of their solid solutions.

The only report on the Raman spectra of optic phonons in mixed Cu halides is that of Murahashi *et al.*[13] It deals with $CuCl_{1-x}I_x$, which shows a two-mode behavior but does not fully mix with $CuBr_{1-x}I_x$, which shows a one-mode behavior, and with $CuCl_{1-x}Br_x$, which is of main concern for the present work and therefore will be dealt with in more detail. On the basis of the Raman spectra recorded at 4 K, Murahashi *et al.* claim that $CuCl_{1-x}Br_x$ shows a two-mode behavior.[13] They refer to the TO(γ)-LO(γ) as the polar mode of CuCl throughout the mixture as one of the modes, and to the TO-LO pair of CuBr as the other. There is nothing unusual about the local Cl mode in CuBr, but the Br gap mode in CuCl accidentally coincides with the β mode of CuCl. Also infrared absorption spectra of $CuCl_{0.90}Br_{0.10}$, and $CuCl_{0.85}Br_{0.15}$ in which two absorption lines appear, are shown by Murahashi *et al.*[13]; one corresponds to CuCl and the other to CuBr.

The other study of phonons in $CuCl_{1-x}Br_x$ concentrates on the Raman disorder-induced TA-phonon line.[9] It is shown there that disorder-induced Raman lines do frequently appear in mixed crystals. The unusual phenomenon specific to the $CuCl_{1-x}Br_x$ system is the high intensity of the TA disorder-induced line, higher than the rest of the spectrum. This is attributed mainly to the high disorder caused by the ability of copper ions to occupy either an ideal or an off-center position in addition to the disorder imposed by the anion mixture.

The motivation behind the present study of optic phonons in $CuCl_{1-x}Br_x$ is twofold: to understand the peculiar behavior of the phonons in this system and by doing that to reexamine our view about the anomalies which occur in pure Cu halides. The new experiments and their results are divided into two main parts. The first one is presented in Sec. II and includes additional Raman data on $CuCl_{1-x}Br_x$ as well as on polaritons in mixed binary systems. The second part is devoted to polaritons

in mixed $CuCl_{1-x}Br_x$ and is described in Sec. III. A general discussion is given in Sec. IV, and its conclusions are summarized in Sec. V.

II. RAMAN DATA ON $CuCl_{1-x}Br_x$ AND POLARITONS IN MIXED BINARY SYSTEMS

A. Raman spectra of $CuCl_{1-x}Br_x$

We reproduced the Raman spectra of $CuCl_{1-x}Br_x$ at low temperatures (2 K) and a few of these are shown in Fig. 1. For $0 < x < 1$ four main lines appear in each spectrum: the upper polar mode labeled TO(2)-LO(2) and the lower one labeled TO(1)-LO(1). In this sense it may be classified as having a two-mode behavior. However, when the line intensity is more carefully examined this assignment does not seem very convincing any longer.

Typically, the scattering line intensity of a one-mode crystal changes gradually from that of one end of the mixture to that of the other end.[14] In a two-mode crystal the intensity of the line characteristic of each component drops gradually to zero with the dilution of that component.[14] Indeed, the intensity of the TO(2)-LO(2) pair which emerges from the γ mode of CuCl does drop to zero with $x \to 1$. Therefore, it exhibits the behavior similar to that found for a two-mode phonon branch in a solid solution. But when the intensity of the other pair is examined, namely, the one which emerges from TO-LO of CuBr, it does not drop to zero for $x \to 1$. With x decreasing from $x = 1$, its intensity decreases relatively to the increase of TO(2)-LO(2) up to $x = 0.40$ (see Fig. 1). But from then on it does not change much and at $x = 0.05$ it is very similar to that of β-CuCl. That is to say that for high Br concentration this mode is characteristic of CuBr and for high Cl concentration it is characteristic of the β mode of CuCl. This intensity variation is thus of a mixed type: that of two mode for the Br-rich solution and semi-one-mode for the Cl-rich solution. It should, however, be noted that this qualitative description serves just to indicate the peculiar concentration-dependent intensity of $CuCl_{1-x}Br_x$.

The frequencies of the Raman lines for the various concentrations are shown in Fig. 2. These data are in essential agreement with those of Murahashi *et al.*[13] There is a minor change in the position of the Cl local mode, which is of higher frequency in the present report. In addition we concentrated on the (1) branch at small values of x in order to obtain more accurate and detailed data in this range. In fact, the frequency shift with concentration in this region is not as smooth

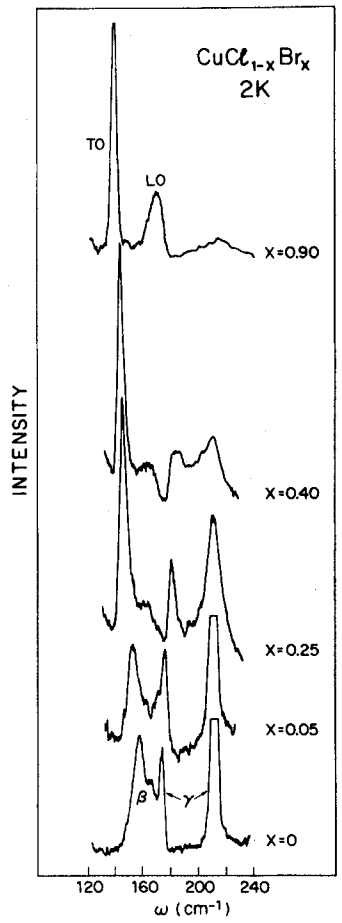

FIG. 1. Raman spectra of $CuCl_{1-x}Br_x$ at 2 K. The TO and LO lines of CuBr and β and γ lines of CuCl are marked.

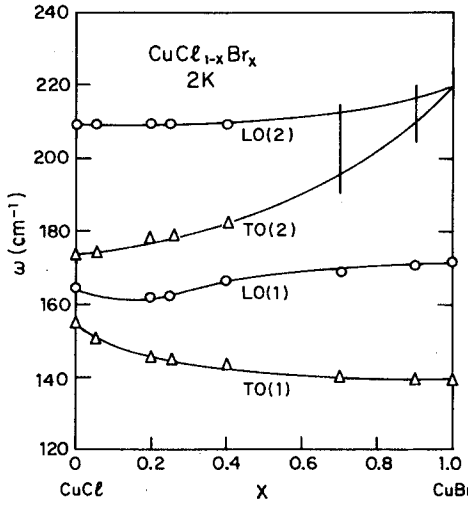

FIG. 2. Frequencies of TO(1)-LO(1) and TO(2)-LO(2) as functions of the concentration. The lines serve as a guide to the eye.

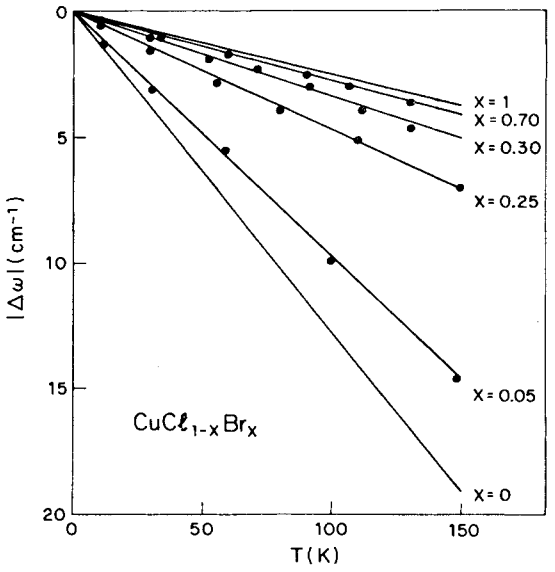

FIG. 3. Frequency shift versus temperature of TO(1) at various concentrations; that of pure CuBr and CuCl are shown for reference.

as in the other concentration regions. One gets the impression of two modes that coincide with regard to frequency, but are not well glued together, which is very similar to the impression one had examining the intensity variation of these lines. Also the Br-rich side of branch (1) does not behave regularly. In a two-mode mixed crystal the frequency separation of the TO-LO modes decreases towards the gap mode. Here the separation is about constant for $0.50 < x < 1$.

Another approach for examining the nature of the phonon lines at the various concentrations is to measure their frequency shift $\Delta\omega$ as a function of temperature. We recorded the Raman spectra of $CuCl_{1-x}Br_x$ at various temperatures between 2 and 150 K. It was found that $\Delta\omega/\Delta T$ of LO(1), TO(2), and LO(2) is small and insensitive to changes of the concentration. In the case of TO(1), $\Delta\omega/\Delta T$ shows little change in the range of $0.40 < x < 1$, where it has approximately the temperature frequency shift of TO of CuBr.[12] From then on ($0 < x < 0.40$) there is an abrupt change of $\Delta\omega/\Delta T$ which finally reaches its highest value, that of TO(β) in CuCl ($x = 0$).[6] This is shown in Fig. 3.

These results seem to indicate that in branch (1), TO(β) of CuCl and TO of CuBr are incorporated. The contribution of TO(β) is significant for $0 < x < 0.40$ and that of TO of CuBr is significant for $0.40 < x < 1$ and there is a region where both contributions are important ($0.20 < x < 0.50$).

We conclude from these preliminary Raman measurements that the behavior of branch (1) is quite anomalous in regard to its intensity, its frequency, and its temperature-dependent frequency shift, as the concentration x of $CuCl_{1-x}Br_x$ is varied.

B. Polaritons in mixed crystals

Measurements of phonon polaritons were successfully used in studying anomalies in pure Cu halides[10]; therefore the same method was applied to $CuCl_{1-x}Br_x$ solid solutions. However, we did not come across polariton measurements in binary mixed crystals. Therefore we checked this method on well known mixed crystals prior to its application to oddly behaved solutions. The candidates for the polariton study were selected according to their relevance to the present research. Therefore we looked for crystals of zinc-blende structure and a single polar mode, which form solid solutions and are experimentally convenient.

In fact, the polariton dispersion curve of any system may be calculated once its infrared reflection spectrum is given or when the TO and LO frequencies together with the dielectric constants ϵ_0 and ϵ_∞ are known. The dispersion is expressed in terms of[15]

$$cq = \omega[\epsilon(\omega)]^{1/2} = \omega\left\{\epsilon_\infty + \sum S_i \Big/ \left[1 - \left(\frac{\omega}{\omega_{\mathrm{TO}(i)}}\right)^2\right]\right\}^{1/2}, \tag{1}$$

where S_i are the oscillator strengths of all polar modes and TO(i) are the frequencies of the corresponding transverse-optic phonons. The frequencies of LO(i) then satisfy $\epsilon(\mathrm{LO}(i)) = 0$. Evaluations of the oscillator strengths in $A\,B_{1-x}C_x$ solid solutions were performed by Chang and Mitra,[16] Genzel[17] *et al.*, and Jahne.[18,19] They obtained an approximate linear dependence of the oscillator strengths on x for one-mode and two-mode solid solutions.

The Raman polariton measurements are perhaps the best way to obtain the dispersion experimentally, and the oscillator strength is then determined with far better accuracy. This is especially true as compared to oscillator strength calculations based on phonon frequencies. We recorded the polariton spectra of $GaP_{0.85}As_{0.15}$ and $ZnS_{0.25}Se_{0.75}$, both two-mode mixed crystals. In the first just the upper polariton dispersion could be followed, while in the latter only the lower polariton lines could be recorded. Nevertheless, one is able to obtain the two-oscillator strengths S_1 and S_2 by fitting the single measured dispersion curve, if, in addition, the large-angle frequencies of the other polar modes are known, and the linearity of $\epsilon_0(x) - \epsilon_\infty(x)$ is assumed. The polariton dispersion measurement of $Zns_{0.25}Se_{0.75}$ is a suitable test for our purpose and is presented together with the cal-

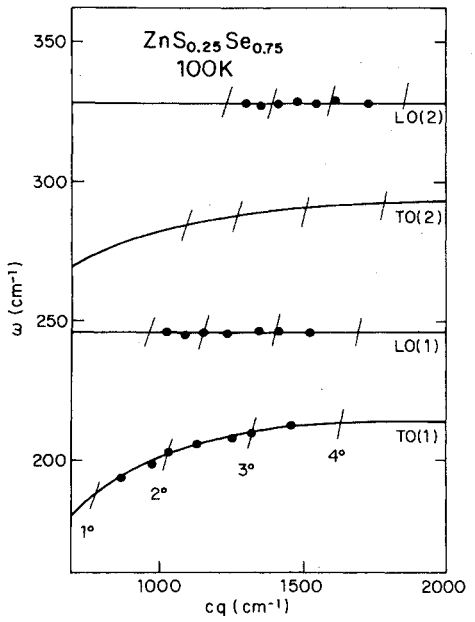

FIG. 4. Polariton dispersion in $ZnS_{0.25}Se_{0.75}$ at 100 K. The full lines are the calculated best fit (see text) to the experimental data (circles).

culated dispersion curves in Fig. 4.

Our polariton data of $Ga_{1-x}In_xP$ could not be fitted by a single oscillator dispersion if one requires that ϵ_0 and ϵ_∞ vary approximately linearly with x. Although in $Ga_{1-x}In_xP$ the polar mode is considered to have a one-mode behavior, a second oscillator is necessary for the polariton fit, no matter how small its strength may be. The polariton data of $Ga_{0.70}In_{0.30}P$ are presented in Fig. 5 along with the two-oscillator fit. The two branches are denoted by (1) and (d), which are the main oscillator and the disorder-induced oscillator, respectively. The ratio $S(1)/S(d)$ is of the order of 20. The high sensitivity of the polariton measurements to extremely small oscillator strengths makes them an important tool for studying the origin of the peculiar behavior of the optic-phonon modes of $CuCl_{1-x}Br_x$.

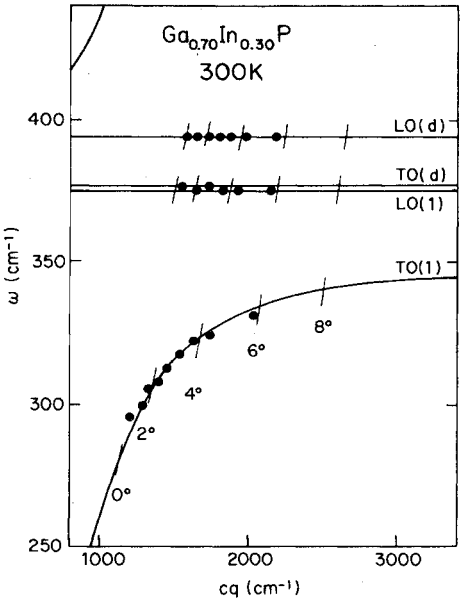

FIG. 5. Polariton dispersion in $Ga_{0.70}In_{0.30}P$ at 300 K. The full lines are the calculated best fit (see text) to the experimental data (circles).

III. POLARITONS IN $CuCl_{1-x}Br_x$

Raman forward-scattering measurements at $T = 11$ K were taken on $CuCl_{1-x}Br_x$ crystals for $x = 0.05$, 0.20, 0.25, 0.40, 0.70, and 0.90. These on pure CuCl ($x = 0$) were taken at 2 K. The polycrystalline samples, grown by the Bridgman technique,[13] had dimensions of a few mm and were very finely polished. The exciting irradiation was a 400-mW, 6471-Å line of a Kr^+ laser and the scattering geometry was that described in Ref. 10. The scattered light was analyzed using a triple spectrometer set with a resolution of 2–3 cm^{-1}.

From the measured angular dispersion of the frequency, $\omega_p = f(\Psi)$, the polariton dispersion is calculated using the relation[15]

$$cq = \left[\omega_p^2\left(n - \lambda\frac{dn}{d\lambda}\right)^2_{\lambda=\lambda_i} + \omega_i^2\Psi^2\right]^{1/2}, \qquad (2)$$

where ω_i is the laser frequency, Ψ is the external angle, and $n(\lambda)$ is the refraction index of the crystal at that wavelength.

The polariton dispersion of CuBr at low temperature was reported earlier,[10] and that of CuCl is shown in Fig. 6. The polariton data of CuCl measured at 2 K can only be fitted to a two-oscillator calculated dispersion curve similarly to the higher-temperature results.[10] The oscillator strengths so obtained were $S_\beta = 1.7$ and $S_\gamma = 0.6$; these values were discussed in detail earlier.[10]

Having the necessary information on CuCl and CuBr, we now turn to deal with the polariton dispersion of $CuCl_{1-x}Br_x$. In all the concentrations of $CuCl_{1-x}Br_x$ only the dispersion of the lowest-frequency polariton branch could be measured. As an example, in Fig. 7 we present spectra of $CuCl_{0.75}Br_{0.25}$ taken at various angles Ψ at $T = 11$ K; the polariton lines are indicated by arrows.

The next step is to fit this experimental polariton dispersion by a functional dependence having the form of Eq. (1). We assume that $\epsilon_0(x)$, $\epsilon_\infty(x)$, and $\{n(x) - \lambda[dn(x)/d\lambda]\}_{\lambda_i}$ vary linearly with x. The straightforward approach would be to calculate the dispersion curves on the basis of frequencies

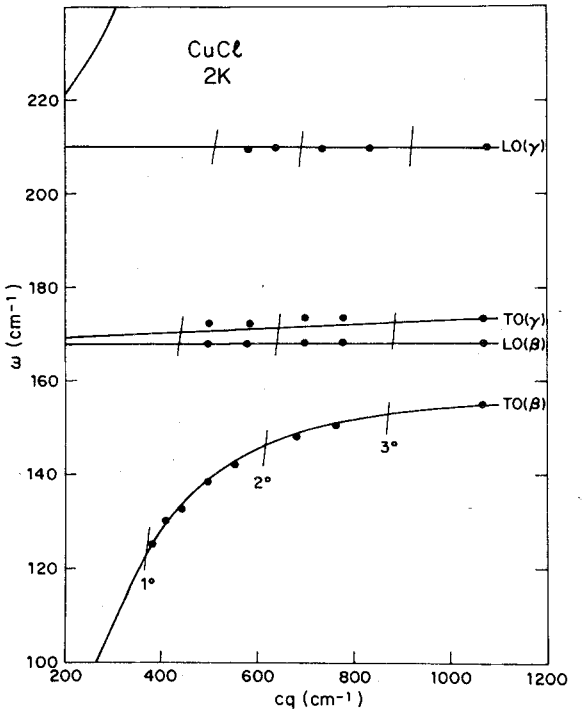

FIG. 6. Polariton dispersion in pure CuCl at 2 K. The full lines are the calculated best fit (see text) to the experimental data (circles).

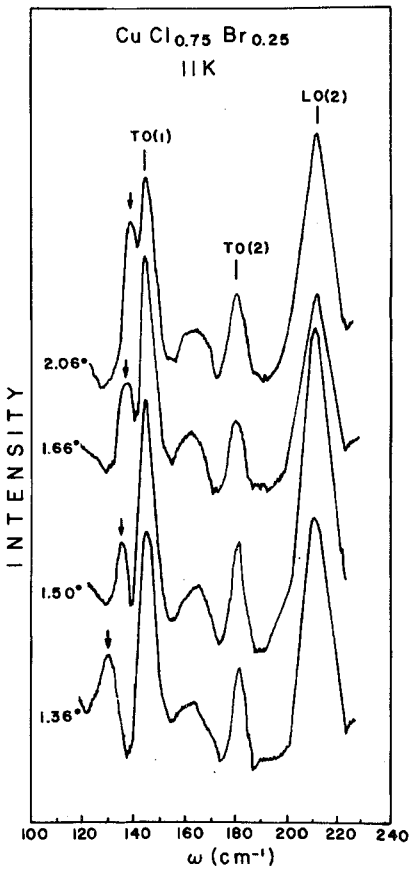

FIG. 7. Polariton spectra of $CuCl_{0.75}Br_{0.25}$ at several external angles Ψ. The polariton lines are marked by arrows.

of the four Raman lines TO(1)-LO(1) and TO(2)-LO(2). This is shown by the dashed line in Fig. 8. The misfit is striking.

An alternative approach is to use the measured TO(1), TO(2), and LO(2) frequencies and obtain S_1 and S_2 in terms of one parameter: LO(1), which is the solution of $\epsilon(\omega_{LO(1)}) = 0$. Now the calculated curve fits the experimental data very well, but using $\omega_{LO(1)}$ as a parameter leads to an unacceptable LO(1) frequency, which is lower than the observed one by 10–15 cm^{-1}. Neither the experimental error nor the neglect of damping can account for this difference. Moreover, the observed LO(1), which can be followed from the LO of CuBr, remains unassigned. Only one way is left to give a meaningful physical interpretation to this line. This is to assume the existence of a third oscillator, and we denote its frequencies and strength by TO(d), LO(d), and S_d, respectively.

Some additional physical assumptions have to be made in order to minimize the number of fitting parameters. First, the Raman spectra indicate a broadening and asymmetry of the LO line of CuBr when introducing Cl, a peculiarity which continues for all x. Therefore, a reasonable assumption would be to consider this line as a double peak, that of TO(d)-LO(d). This also satisfies the second requirement that S_d will be relatively small.

Thus we are finally led to a three-oscillator model, with two fitting parameters: LO(1) and TO(d). The dispersion calculated this way is shown in Fig. 8 for $CuCl_{0.75}Br_{0.25}$ (full lines); the circles represent the measured values of the lowest-frequency branch.

We get the three-oscillator strengths S_1, S_2, and S_d as functions of x, and these are drawn in Fig. 9 together with the values of S_β, and S_γ in CuCl ($x = 0$) and S of CuBr ($x = 1$). The corresponding frequencies TO(1)-LO(1), TO(d)-LO(d), and TO(2)-LO(2) are drawn in Fig. 10.

It is true that the full dispersion curve can be obtained by fitting the single measured branch; we proved it for $ZnS_{1-x}Se_x$ and $GaP_{1-x}As_x$. However, the question still remains: Why is the rest of the polariton branches not measurable? In order to answer this question the Raman efficiency[15] for $CuCl_{0.75}Br_{0.25}$ was calculated and it is presented in Fig. 11. First of all it is obvious that the line intensity of the lower polariton is larger than

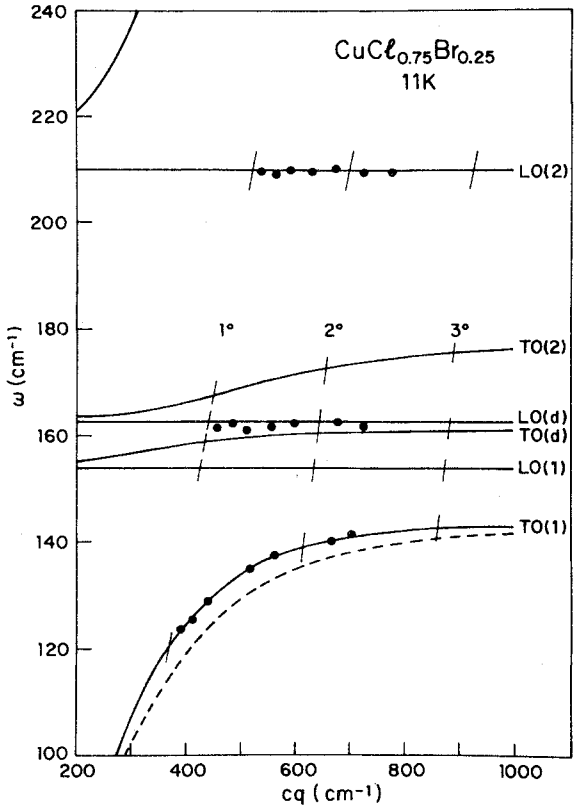

FIG. 8. Polariton dispersion in $CuCl_{0.75}Br_{0.25}$ at 11 K. The full lines are the calculated best fit (see text) to the experimental data (circles). The dashed line is the calculated polariton dispersion based on two oscillators (see text).

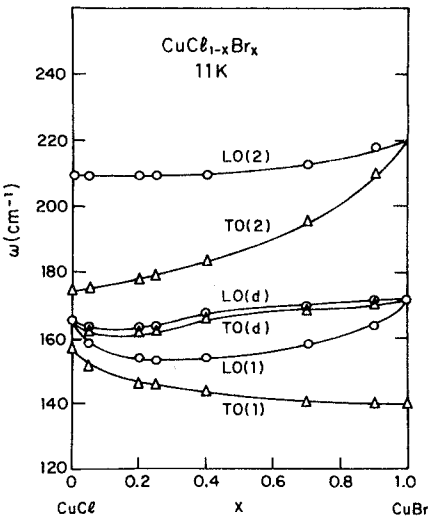

FIG. 10. Frequencies of TO(1)-LO(1), TO(d)-LO(d), and TO(2)-LO(2) which correspond to S_1, S_d, and S_2 of Fig. 9 at various concentrations.

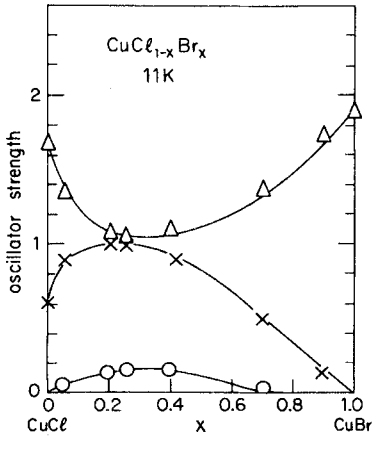

FIG. 9. Three-oscillator strengths S_1, S_2, and S_d (triangles, crosses, and circles, respectively) for the various concentrations at 11 K. The lines serve only as a guide to the eye.

that of the other polariton branches, even for large angles Ψ. Moreover, at large Ψ the polariton lines are unresolved from their corresponding TO lines. Therefore, when the intensities are compared in the Ψ region of interest, namely $1° < \Psi < 2°$, the only measurable polariton line is that of the lower-frequency branch, while the rest are undetectable.

IV. DISCUSSION

In the last section we described the experimental results and the procedure which enabled us to present the data in terms of three-oscillator

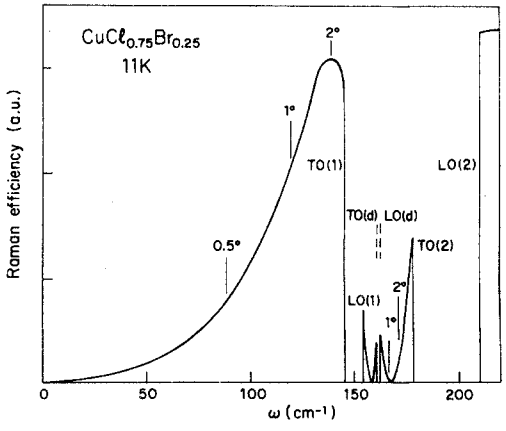

FIG. 11. Calculated Raman efficiency as function of frequency for $CuCl_{0.75}Br_{0.25}$ at 11 K. Angles of interest for polariton scattering efficiency are indicated.

strengths as a function of the concentration (Fig. 9). As a matter of fact, there are two main oscillator strengths S_1 and S_2 (S_d is relatively small and is ignored for the moment); therefore the crystal could be described as having a two-mode behavior. But their variation with x is by no means similar to that expected for a two-mode mixed crystal (see Sec. II B). If the TO(1) is considered to originate from the TO of CuBr then its oscillator strength should decrease with decreasing Br concentration, which indeed happens for $0.30 < x < 1$. But from then on until $x = 0$, S_1 keeps growing. On the other hand, if S_2 represents the CuCl contribution, instead of decreasing when Br is introduced ($0 < x < 0.20$), S_2 is growing. Only when $x > 0.20$ does S_2 begin to decrease and finally tend to zero when approaching pure CuBr.

Contrary to that, the two-oscillator strengths vary quite linearly with x at the Br-rich end. Moreover, the slope of S_1 is such as to become zero at $x = 0$ as expected, while that of S_2 is such that linear extrapolation would result in $S_2(0) \approx 2$ for pure CuCl, which is quite reasonable: The total oscillator strength of CuCl is $S_\beta + S_\gamma = 2.3$.

The described behavior places the irregularities at the Cl-rich side. This is not unexpected in light of the anomalies which are known to exist in CuCl at low temperatures. Therefore let us focus first on CuCl, in which the existence of two polar phonon modes is well established by Raman, infrared, and neutron scattering spectroscopy.[1-10] We shall leave aside for the moment the controversial explanations given to this anomaly and concentrate on the experimental facts, namely the existence of two polar modes in CuCl and only one in CuBr ($T = 11$ K), all three having the same symmetry.

The picture we are trying to draw is that of an essentially two-mode behavior of the $CuCl_{1-x}Br_x$ mixed crystal. If one assigns one mode to CuCl and the other to CuBr, and if one keeps in mind that the oscillator strength is proportional to the number of "oscillators" participating in a given mode, then both S_1 and S_2 should gradually decrease with the mixing of the two crystals. But evidently S_2 gains strength very fast at low values of x while at the same time S_1 is losing strength at almost the same rate. We shall look for the various contributions to $S_1(x)$ and $S_2(x)$ and for a mechanism which would be capable of pumping strength from S_1 to S_2 as x grows. We know that this mechanism which triggers the odd behavior of phonons in $CuCl_{1-x}Br_x$ ought to decay very fast with x; what is that mechanism?

We argue that the model which allows Cu ions to occupy off-center sites[8-10] is adequate to explain the present results. At low temperature (11 K) a substantial percentage of the copper ions in CuCl occupy off-center sites yielding the β mode and its high oscillator strength. The copper ions in CuBr occupy ideal sites only. From a microscopic point of view the mixed crystal can be considered to be composed of five types of tetrahedera based on n chlorine ions and $4 - n$ bromine ions, where $0 \leq n \leq 4$. When randomly distributed, the probability of each type is easily calculated for a given concentration x.[20]

The assumptions we choose are meant to yield a minimum number of parameters in order to check the physical basis of our model. That is why we neglect the possibility of clustering in the $CuCl_{1-x}Br_x$ solid solutions. Our fundamental assumption is that at low temperatures, only Cu^+ in tetrahedra built exclusively of chlorine ions ($n = 4$) may occupy off-center positions and that this happens with the same probability as in pure CuCl. In tetrahedra with $n \neq 4$, Cu^+ occupy central positions only. The probability of tetrahedra with $n = 4$ to occur is $f = (1 - x)^4$. When $S_\beta = 1.7$ is weighed by this probability, the contribution of CuCl to $S_1(x)$ is found. We denote this contribution by $S_\beta(x)$ and find $S_\beta(x) = 1.7(1 - x)^4$. This result is shown by the dotted curve in Fig. 12. The other contribution to $S_1(x)$ comes from the polar mode of CuBr. Its oscillator strength is assumed to vary linearly with x, the thin line in Fig. 12. The two-oscillator strengths add up to what should be $S_1(x)$, the heavy line in Fig. 12.

We assume that the total oscillator strength of the polar modes of CuCl decreases linearly with x (S_{CuCl}, the thin line in Fig. 12). From S_{CuCl}, the experimentally obtained $S_d(x)$ is subtracted,

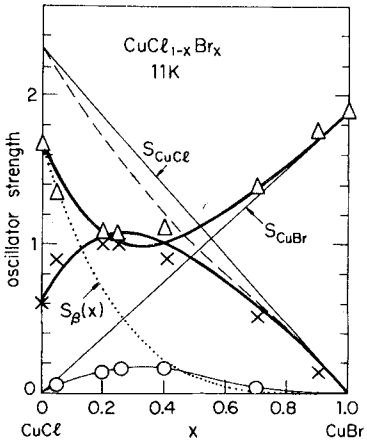

FIG. 12. Layout of the functions used for deducing the $S_1(x)$ and $S_2(x)$ (heavy lines). S_{CuCl}, S_{CuBr}, and $S_d(x)$ are indicated and are explained in the text. The dashed line is $S_{CuCl} - S_d$. The triangles, crosses, and circles are the S_1, S_2, and S_d values, respectively, deduced from the polariton data and are the same as in Fig. 9.

relating $S_d(x)$ mainly to CuCl. This will be justified later in this section. The dashed line in Fig. 12 is the result $S_{CuCl}(x) - S_d(x)$ and it represents the sum of two contributions: that of $S_\beta(x)$ and $S_\gamma(x)$. Therefore, subtracting $S_\beta(x)$ from the dashed line yields $S_2(x) = S_\gamma(x)$, which is indicated in Fig. 12 by a heavy line. It should be emphasized that the oscillator strength missing from $S_1(x)$ due to the decrease in $S_\beta(x)$ (as Cu^+ move from off-center sites to central sites) reappears in $S_2(x)$.

The heavy lines in Fig. 12 are the calculated values of $S_1(x)$ and $S_2(x)$; the triangles and crosses are the corresponding experimental values obtained from the polariton measurements. Considering the fact that the only parameters we used were those employed in fitting the polariton data, the fit is surprisingly good. This shows that the model used is self-consistent and, in addition, it gives reasonable solutions to the problems which were presented earlier.

First of all, it explains the odd way in which the oscillator strengths S_1 and S_2 vary as functions of the concentration x. It also explains the intensity of TO(1) as a function of x: The TO(1) line represents the contribution of CuBr which depends on x, and of the β line of CuCl, which is proportional to $(1-x)^4$. Therefore TO(1) becomes more intense as either of the extreme cases $x \to 0$ and $x \to 1$ is approached.

The temperature dependence of the TO(1) frequency for various concentrations can also be deduced now. For a wide range of x $(0.30 < x < 1)$ one deals with a dependence similar to that of CuBr. This happens as long as the Cu^+ off-center population is sufficiently small. It is only when the probability of finding Cu^+ at off-center sites (dotted curve) becomes significant, namely, at small values of x (for $0 < x < 0.30$) that this dependence changes, and becomes similar to that of the β line of CuCl.

Finally, we discuss the third oscillator. Its strength is small compared to the other two oscillators at all concentrations. The fact that S_d was subtracted from S_{CuCl} alone has a negligible overall effect. However, it is assumed that S_d is the result of disorder. So it is affected also by the ability of the Cu ions to occupy off-center as well as central sites.

In one-mode-type crystals such as $Ga_x In_{1-x} P$ (Ref. 21) and $Cd_x Zn_{1-x} S$,[18] disorder-induced polar lines were found; their oscillator strengths were also one order of magnitude smaller than that of the main polar mode. There the maximum of $S_d(x)$ was found at $x \approx 0.50$. In the case of $CuCl_{1-x}Br_x$ the maximum of S_d is shifted towards smaller values of x, where the Cu^+ disorder is more effective. Therefore it seems natural to relate it mainly to S_{CuCl}.

V. CONCLUSIONS

We presented and discussed the peculiar behavior of the optical-phonon spectrum in $CuCl_{1-x}Br_x$ with respect to a number of phenomena. This mixed crystal has basically two polar modes but the Raman intensity, the frequency, and the temperature-induced frequency shift as functions of concentration are not those characteristic of a two-mode behavior. The anomalies are striking particularly in the low-frequency mode and limited to the chlorine-rich end. The fit of the Raman polariton spectra yielded a complicated picture in which three oscillators are involved. One of these oscillators has relatively small strength, S_d, and the other two, S_1 and S_2, exhibit a peculiar concentration dependence especially in the region $0 < x < 0.40$.

The interpretation of all these phenomena starts with the anomaly of the second polar mode (β) in CuCl. It is claimed that the lower polar mode (1) consists of two contributions: that of CuBr and that of β-CuCl. The contribution of β-CuCl decays very fast with concentration, corresponding to the decrease in the concentration of "all-chlorine" tetrahedra in the mixed crystal. We employed here our model,[8] which relates the appearance of β-CuCl to the presence of copper ions at off-center sites and assumed that this may occur only in all-chlorine tetrahedra. This enabled us to calculate the concentration dependence of the two main oscillator strengths, $S_1(x)$ and $S_2(x)$. The calculated curve satisfactorily fits the experimental results.

This interpretation helps also to understand the other peculiar phenomena reported here, namely, the unusual high intensity of the TO(1) line for $0 < x < 0.40$ and the concentration dependence of the temperature-induced frequency shift of this line. Moreover, we believe that the present work supports the model reported previously[8-10] for the anomalous phonon spectrum of the Cu halides.

ACKNOWLEDGMENTS

We wish to thank Dr. S. Suga for supplying the $CuCl_{1-x}Br_x$ crystals and to H. Katz for most valuable technical assistance.

*Present address: Division of Engineering, Brown University, Providence, Rhode Island 02912.

[1]A. Hadni, F. Brehat, I. Claudel, and P. Strimer, J. Chem. Phys. 49, 471 (1968).
[2]I. P. Kaminow and E. M. Turner, Phys. Rev. B 5, 1564 (1972).
[3]J. E. Potts, R. C. Hanson, C. T. Walker, and C. Schwab, Phys. Rev. B 9, 2711 (1974).
[4]B. Hennion, B. Prevot, M. Krauzman, R. M. Pick, and B. Dorner, J. Phys. C 12 (1609), 1979.
[5]M. Krauzman, R. M. Pick, H. Poulet, G. Hamel, and B. Prevot, Phys. Rev. Lett. 33, 528 (1974).
[6]T. Fukumoto, S. Nakashima, K. Tabuchi, and A. Mitsuishi, Phys. Status Solidi B 73, 341 (1976).
[7]M. L. Shand, H. D. Hochheimer, M. Krauzman, J. E. Potts, R. C. Hanson, and C. T. Walker, Phys. Rev. B 14, 4637 (1976).
[8]Z. Vardeny and O. Brafman, Phys. Rev. B 19, 3276 (1979).
[9]Z. Vardeny and O. Brafman, Phys. Rev. B 19, 3290 (1979).
[10]Z. Vardeny and O. Brafman, Phys. Rev. B 21, 2585 (1980).
[11]E. M. Turner, I. P. Kaminow, and C. Schwab, Phys. Rev. B 9, 2524 (1974).
[12]J. E. Potts, R. C. Hanson, and C. T. Walker, Solid State Commun. 13, 389 (1973).
[13]T. Murahashi and T. Koda, J. Phys. Soc. Jpn. 40, 747 (1976).
[14]*The Raman Effect*, edited by A. Anderson (M. Dekker, New York, 1973).
[15]R. Claus, L. Merten, and J. Brandmuller, *Light Scattering by Phonon-Polaritons*, Springer Tracts in Modern Physics (Springer, Berlin, 1975).
[16]I. F. Chang and S. S. Mitra, Phys. Rev. 172, 924 (1968).
[17]L. Genzel, T. P. Martin, and C. H. Perry, Phys. Status Solidi B 62, 83 (1974).
[18]E. Jahne, Phys. Status Solidi B 74, 275 (1976).
[19]E. Jahne, Phys. Status Solidi B 75, 221 (1976).
[20]H. V. Verleur and A. S. Barker, Jr., Phys. Rev. 149, 715 (1966).
[21]E. Jahne, W. Pilz, M. Giehler, and L. Hildisch, Phys. Status Solidi B 91, 155 (1979).